https://doi.org/10.5194/egusphere-2022-1368
Preprint. Discussion started: 19 December 2022

Seasonal Sea Ice Prediction with the CICE Model and Positive Impact of CryoSat-2 Ice Thickness Initialization

Shan Sun[1] and Amy Solomon[2]

[1]NOAA/Global Systems Laboratory, USA
[2] University of Colorado Boulder, Cooperative Institute for Research in Environmental Sciences and NOAA/Physical Sciences Laboratory, USA

Correspondence: Shan.Sun@noaa.gov

Abstract. The Los Alamos sea ice model (CICE) is being tested in standalone mode to identify biases that limit its suitability for seasonal prediction. The prescribed atmospheric forcings to drive CICE are from the NCEP Climate Forecast System Reanalysis (CFSR). A built-in mixed layer ocean model in CICE is used. Initial conditions for the sea ice and the mixed layer ocean are also from CFSR in the control experiments. The simulated sea ice extent is generally in good agreement with observations in the warm season at all lead times up to 12 months both in the Arctic and Antarctic, suggesting that CICE is able to provide useful sea ice edge information for seasonal prediction. However, the Arctic sea ice thickness forecast has a positive bias stemming from the initial conditions, and this bias often persists for more than a season, limiting the model's seasonal forecast skill. When this bias is reduced by initializing ice thickness using the CryoSat-2 satellite observations while keeping all other initial fields unchanged in the CS2_IC experiments, both simulated ice edge and thickness improve. This confirms the important roles of sea ice thickness initialization in sea ice seasonal prediction seen in many studies.

1 Introduction

Sea ice concentration observations from passive microwave satellites show that ice coverage has decreased rapidly in the Arctic in recent decades, a region presently with the greatest warming on earth (Chapman and Walsh, 2003; IPCC, 2014). Global climate models suggest that further reduction in sea ice coverage and thickness will occur in the coming decades (e.g., IPCC, 2014, 2021). Sea ice in the polar oceans has a major impact not only on the regional energy balance but on the global climate as well. A relatively thin material layer between the atmosphere and ocean, sea ice amplifies radiative feedback with a higher surface albedo than open water (e.g., Holland and Bitz, 2003; ACIA, 2005; Dethloff et al., 2006). Thus, changes in sea ice are one of the most sensitive and visible indicators of our changing climate. Reliable sea ice prediction is important not only for the polar regions but also is expected to improve predictability in mid-latitudes at subseasonal to seasonal (S2S) time scales due to teleconnections (e.g., Randall et al., 1998; Jaiser et al., 2012; Li et al., 2014).

Finding sources of weather predictability at S2S time scales is a challenging research topic. Sea ice is found to be one candidate due to the persistence of seasonal anomalies (Blanchard-Wrigglesworth et al., 2011a; Holland et al., 2011; Bushuk et al., 2019). Much progress has been made on sea ice modeling in recent decades, which holds promise for improving both medium-range and climate predictions (e.g., Wang et al., 2013; Hebert et al., 2015; Guemas et al., 2016; Chevallier et al.,

https://doi.org/10.5194/egusphere-2022-1368
Preprint. Discussion started: 19 December 2022

2017). Weather predictions from a numerical model incorporating a sea ice model are found to have a higher skill than those based on persistence of Arctic sea ice (Grumbine, 2003; Hebert et al., 2015; Intrieri et al., 2022). In addition, the predictive skill for sea ice forecasts at seasonal to interannual time scales relies on the accuracy of the sea ice initial conditions (Holland et al., 2011; Blanchard-Wrigglesworth et al., 2011b; Wang et al., 2013) and, in particular, the fidelity of sea ice thickness initialization, as thickness has more persistence than ice-covered area (Krinner et al., 2010; Chevallier and Salas-Mélia, 2012; Day et al., 2014a; Collow et al., 2015; Allard et al., 2018; Blockley and Peterson, 2018; Schröder et al., 2019, to name a few). It has also been shown that sea ice predictability is season-dependent (Holland et al., 2011; Day et al., 2014b; Bushuk et al., 2020), and that predictability of minimum sea ice extent depends on atmospheric spring and early summer conditions where inclusion of melt ponds is seen to make a difference (Liu et al., 2015; Schröder et al., 2019; Bushuk et al., 2020).

A fully coupled atmosphere-ocean-sea ice model is considered the ultimate tool for sea ice prediction at seasonal and climate time scales (e.g., IPCC, 2014, 2021). We chose the Los Alamos Community Ice CodE (CICE; Hunke et al., 2015) as the sea ice model in this study, due both to its popularity in the community (e.g., Holland et al., 2011; Roberts et al., 2015; Hunke et al., 2020; Intrieri et al., 2022) and to the fact that it is being incorporated into NOAA's Unified Forecast System (UFS) which is to be NOAA's next operational coupled atmosphere-ocean-seaice-land system for S2S predictions. In order to separate various feedbacks among components of a fully coupled model, in this study we aim to identify the model biases that limit the seasonal prediction skill of CICE in standalone mode with prescribed atmospheric forcings. It is informative to assess the skill of each module separately in uncoupled mode before assembling them in a fully coupled model, as only in such a controlled environment it is possible to reveal the strength and weakness of an individual module. This work is even more relevant as CICE, originally developed for climate research, is to be used in operational S2S prediction. We hope to build a set of baseline sea ice forecasts for future studies including coupled models using this sea ice module. We also investigate the sensitivity of forecast skill when the bias in the sea ice thickness initialization is reduced. The detailed experimental setup is described in section 2. Its basin-wide and regional performance at different lead times, as well as with different initializations, are presented in section 3, followed by a discussion in section 4.

2 Model Setup

CICE is a dynamic–thermodynamic sea ice model designed for application in global climate models. We adopted the CICE code V5.1.2 (Hunke et al., 2015) in this study, where the linear function of salinity was used for the freezing temperature (ktherm=1), the elastic-viscous-plastic rheology were specified for the sea ice dynamics (kdyn=1) and the ice strength was set to be closely related to the ridging scheme (kstrength=1). In addition, CICE needs the information of sea surface temperature (SST) which can be either prescribed or generated by its built-in mixed layer model. We chose the latter in this study for the sake of consistency between the SST and the ice state.

A combination of an Arctic bipolar grid projection and a Mercator projection of the rest of the globe (Fig.1 in Bleck and Sun, 2004) is used to carry out all CICE experiments. It has a horizontal resolution of 15 km at the North Pole and 30 km at 60°N

https://doi.org/10.5194/egusphere-2022-1368
Preprint. Discussion started: 19 December 2022

and 60°S. The bathymetry from ETOPO1 data (Amante and Eakins, 2009) is interpolated onto the model's global compound grid. A time step of 900 seconds is used in all model experiments.

2.1 Atmospheric Boundary Conditions

The atmospheric boundary forcings are based on the 6 hourly archives from CFSR[1] (Saha et al., 2010). They include downward surface radiation of both shortwave and longwave, 10 m wind, 2 m temperature, 2 m specific humidity, and precipitation (broken down into rain and snow) at 0.2° resolution from 2011 to 2017. These fields were interpolated horizontally onto the compound model grid in a pre-processing step.

2.2 Initial Conditions

In the control experiments, data from the CFSR reanalysis were used as initial conditions for both the ice and the ocean states. These include sea ice concentration and sea ice thickness at 0.2° resolution, sea surface temperature and sea surface salinity at 0.5° resolution. All of these data were interpolated onto the compound model grid at the initial stage.

Monthly mean estimates of Arctic ice thickness are available from the CryoSat-2 satellite observations during boreal winter (October to April) since 2011 (Laxon et al., 2013; Ricker et al., 2014; Grosfeld et al., 2016). This made it possible to carry out additional CICE experiments by initializing ice thickness with this dataset instead of CFSR, despite the large uncertainty in the CryoSat-2 ice thickness when the ice is thinner than 1 m as showed in Ricker et al. (2017) because no other datasets were available. The remaining initial conditions, including snow depth over sea ice as well as atmospheric boundary conditions, are the same as in the control experiments. This set of experiments with an alternative CryoSat-2 ice thickness initialization is called the CS2_IC experiments.

Note that there is no ice thickness available near the North Pole in the original CryoSat-2 dataset. We filled this unphysical hole by interpolating the surrounding ice thickness before using it as the model's initial condition. Ice thickness from CryoSat-2 was treated as one ice thickness category at each grid point in the CICE initialization. Since the CryoSat-2 data are only available in the Arctic, the initial Antarctic sea ice thickness still comes from CFSR in the CS2_IC experiments. In addition, during initialization at grid points with either sea ice concentration (%) in CFSR or sea ice thickness (m) in CryoSat-2 less than 1.e-6, both were reset to zero initially as a temporary solution in order to have a consistent sea ice concentration and sea ice thickness to start with.

The control experiments were initialized at the beginning of each month from April 2011 to December 2017. The CS2_IC experiments initialized with the CryoSat-2 Arctic ice thickness were carried out monthly in the boreal cold season (October to April) from 2011 to 2017, as shown in Table 1. The integration time was 12 months throughout all model experiments.

[1] available at http://rda.ucar.edu/datasets/ds094.0

https://doi.org/10.5194/egusphere-2022-1368
Preprint. Discussion started: 19 December 2022

3 Model Results and Verification

All comparisons and verifications in this section are carried out on the native grid, except for overall evaluations at the hemispheric or regional scales. All fields shown are monthly averages centered on the stated lead time. Lead times not ending on ".5" refer to the month following the stated time.

3.1 Hemispheric Scales

Sea ice extent (SIE) is defined as the area of ocean with at least 15% of sea ice cover, which is a good approximation of the sea ice edge. The simulated SIE and sea ice volume (SIV) in the Arctic and Antarctic in the control experiments are shown in Fig. 1 at lead times of 0.5-month (1st-month average) and 5.5-month (6th-month average) for each target month, together with the SIE from the National Snow and Ice Data Center (NSIDC), which is based on passive microwave satellite sensors (Meier et al., 2012), and SIV observations from CryoSat-2 and SIV reanalysis from the Pan-Arctic Ice Ocean Modeling and Assimilation System (PIOMAS, Schweiger et al., 2011). The lines are averages of 2011-2017 marked with the standard deviation during this time period. The Arctic SIE forecast in Fig. 1(a) matches the NSIDC observations better in the warm season than in the cold season both at 0.5-month and 5.5-month lead times. The modeled interannual variabilities in the Arctic SIE as shown by the standard deviation appear to be similar in all seasons and match those in NSIDC well. In Fig. 1(b), the Arctic SIV forecast at 0.5-month lead time is similar to CryoSat-2 observations or PIOMAS reanalysis in the warm season and is higher than the latter two in the cold season. However, the biggest positive bias in SIV at 5.5-month lead time is shifted to the warm season, suggesting that the bias in the SIT initialization in the cold season lasted for more than a season. The increasing model bias in SIE and SIV with lead time beyond seasonal time scale clearly sets limits for the standalone CICE model in the seasonal application.

The modeled Antarctic SIE in Fig. 1(c) has a positive bias in almost all seasons at 0.5-month lead time compared to the NSIDC observations, where the biggest bias occurs in austral spring, similar to the Arctic. A bigger positive SIE bias is seen in austral spring at 5.5-month lead time. The interannual variabilities in the Antarctic SIE are in general larger than those in the Arctic, both in models and observations. The modeled Antarctic SIV in Fig. 1(d) has a minimum/maximum in February/September at 0.5-month lead time, compared to March/October at 5.5-month lead time. The delay of the minimum/maximum peak at a longer lead time, similar to what happened in the Arctic, indicates a bias in the modeling system which we are unable to narrow down without Antarctic SIV observation or reanalysis. The fact that a bigger SIE bias in the Antarctic than in the Arctic might be the results of the rudimentary ocean representation in the mixed-layer ocean model used in the standalone setup.

To further quantify the forecast skill for the standalone CICE, the root mean square error (RMSE) in the Arctic SIE against the NSIDC observations is shown in the upper panel of Fig. 2 for the control and CS2_IC experiments for each target month at lead times up to 12 months and the difference between the two model experiments. All are averages over the period 2011-2017. White spaces indicate no model data due to lack of the CryoSat-2 data for model initialization from May to September. In the control experiments, the lowest RMSE in the Arctic SIE is in summer and fall at all lead times up to 12 months and

https://doi.org/10.5194/egusphere-2022-1368
Preprint. Discussion started: 19 December 2022

Table 1. Details in two sets of CICE experiments.

Experiments	Atm Boundary Conditions	Initial Conditions for Ice & Ocean	Initialization Months
Control Runs	CFSR	CFSR	Apr 2011 – Dec 2017
CS2_IC Runs	CFSR	Same as in control, except initializing the Arctic with CryoSat-2 ice thickness	Oct-Apr 2011-2017

the biggest RMSE is in late winter and early spring at lead times longer than 3 months. In the CS2_IC experiments when the model is initialized with the CryoSat-2 ice thickness, the RMSE in the Arctic SIE is reduced at different magnitudes in almost all seasons.

The lower panel of Fig. 2 is similar to the upper one, except for SIV with respect to the PIOMAS reanalysis. The control experiments started with a SIV higher than PIOMAS in all months, and a positive SIV bias remained at different magnitudes for all target months at most lead times. The most obvious bias in SIV is the 'summer barrier' in Fig. 2(d), where the reemergence of skill at a longer lead time prior to the winter initialization can be seen clearly. This barrier as well as the overall positive bias in SIV is much reduced in the CS2_IC experiments with the CryoSat-2 ice thickness initialization as shown in Fig. 2(e), where the biggest reduction in the SIV bias is in summer and fall with winter and spring initializations in Fig. 2(f).

Despite a broad reduction in the magnitude of the biases in the SIE and SIV prediction from the CryoSat-2 ice thickness initialization, the bias pattern in the CS2_IC experiments remains similar to that in the control experiments, i.e., the biggest bias in SIV in the warm season as well as the biggest bias in SIE in the cold season, both at 4-7 month lead times. This could be related to the uncoupled experimental setup, where the oceanic heat transport is missing and the prescribed boundary conditions, for both atmosphere and ocean, may not be accurate. Another possible source for biases could be in the CryoSat-2 dataset where relative uncertainties are large over thin ice regimes since sea ice thickness is determined by the ice surface above the sea level (Ricker et al., 2017).

The RMSE in the Antarctic SIE is shown in Fig. 3 for the control experiments with respect to the NSIDC observations in 2011-2017. The SIE forecasts are in good agreement with observations at all lead times for austral summer and especially fall when SIE reaches its annual minimum. The highest RMSE in seasonal forecast occurred in austral spring at its annual maximum, similar to that in the Arctic. There is an austral 'spring barrier' in skill with austral fall and winter initialization in the Antarctic, similar to the 'summer barrier' seen in the Arctic.

3.1.1 Pan-Arctic forecasts at 6-month lead time

In order to investigate the evolution of sea ice distribution, the Arctic sea ice concentration (SIC) in the control and CS2_IC experiments is shown in Fig. 4 during initialization on April 1, 2016, its forecast for October 2016 and the corresponding AMSR2 satellite observations (Spreen et al., 2008). The initial SIC in both experiments is very close to AMSR2. At month 6, a positive SIC bias appeared mostly in the Beaufort, Chukchi and East Siberian Seas in the control experiments, while SIC from the CS2_IC experiments is closer to AMSR2. One reason for this is the difference in sea ice thickness (SIT) shown in

https://doi.org/10.5194/egusphere-2022-1368
Preprint. Discussion started: 19 December 2022

Fig. 5 from the same experiments in Fig. 4. The control experiment started with an ice up to 3 m thicker than the CryoSat-2 observations in the region poleward of the Beaufort and Chukchi Seas in the springtime, and a positive SIT can still be seen 6 months later in this region (lower left panel).

As seen in Figs. 4 and 5, a positive bias in SIT in the initial conditions appears to be one source of the error in SIT as well as SIC in the seasonal forecast. Both SIT and SIC forecasts improved when this initial bias was reduced in the CS2_IC experiment. The positive impact on the forecast skill from a realistic sea ice thickness initialization shown here is consistent with previous findings (e.g., Day et al., 2014a; Collow et al., 2015; Dirkson et al., 2017; Allard et al., 2018; Blockley and Peterson, 2018; Schröder et al., 2019).

3.1.2 Pan-Arctic 12-month forecasts

Fig. 6 presents the SIT in the initial conditions on January 1, 2016, its forecast for December 2016 in both control and CS2_IC experiments and the corresponding CryoSat-2 observations. Similar conclusions can be drawn here as in Fig. 5, i.e., erroneous ice thickness seen in the Beaufort, Chukchi and East Siberian Seas in the 12-month forecast in the control experiment can be traced back to the positive bias in SIT in the initial condition. The SIT forecast for the same time in the CS2_IC experiment is much closer to the CryoSat-2 than in the control. Nevertheless, there is a positive bias in SIT in the Greenland Sea and central Arctic in the CS2_IC experiment. This may be related to the missing northward heat transport from the Atlantic Ocean in the experimental setup where a simplified column mixed layer ocean model is used as mentioned earlier. It could be caused by the prescribed atmospheric forcings as well.

To explore the mechanism behind the difference between the two model experiments seen in Fig. 6, the simulated Arctic SIE and SIV throughout the 12-month integrations are shown in Fig. 7(a) and (b) as well as their comparison to SIE observations from NSIDC and SIV reanalysis from PIOMAS. The initial Arctic SIE in January in both experiments is similar and both are higher than the NSIDC observations. The initial Arctic SIV in the CS2_IC experiment is lower than that in the control experiments and is closer to PIOMAS reanalysis. Both SIE and SIV forecasts in fall in the CS2_IC experiment end up closer to NSIDC and PIOMAS than in the control experiment. The transitions of SIE and SIV from spring to fall are different in these two experiments, which can be traced back to the area and volume tendencies stemming from the thermodynamics and dynamics[2] in the model archives. The tendency averages north of 67.5°N are shown in Fig. 7(c), where there are more thermodynamics-linked tendencies in both ice area and ice volume than the dynamics-linked ones. The negative tendencies in the CS2_IC are slightly bigger than those in the control experiments during the warm season. Furthermore, Fig. 7(d) shows the averaged melting rates from snow, top, basal and lateral, respectively, in both experiments, also north of 67.5°N. The snow melting rate peaks one month earlier than the rest rates. In July, the top melting rate is about twice as big as that from the basal melt. The biggest difference in these melting rates between the two experiments is in the basal melt. The CS2_IC experiment with a higher basal melting rate during summer ended up with both SIE and SIV closer to observations in fall, compared to the control experiment.

[2]In the CICE archives, the variable names for area tendencies from thermodynamics and dynamics are 'daidtt' and 'daidtd', and 'dvidtt' and 'dvidtd' represent volume tendencies from thermodynamics and dynamics, respectively.

https://doi.org/10.5194/egusphere-2022-1368
Preprint. Discussion started: 19 December 2022

To further assess how the melting rate is so different in these two model experiments, the simulated ice concentration and thickness are shown in the left column in the control experiment in Fig. 8. The differences between the CS2_IC and control experiments in the sea ice concentration, sea ice thickness, the top and basal melting rates are shown in the middle and right columns. All are forecast for July 2016 initialized on January 1, 2016. One dominant feature between 120°E and 120°W is that both ice concentration and thickness in the CS2_IC experiment are smaller than those in the control experiment. This is consistent with a higher melt rate both at top and bottom in the marginal ice zone in the CS2_IC experiments, which appears to be more realistic than in the control experiments.

In summary, the seasonal prediction of the Arctic SIE with the CICE model has a higher skill in the warm season than in the cold season at almost all lead times in the control experiment. The biggest Arctic SIT bias is in summer at 3- to 6-month lead times, and in fall/winter at roughly 6- to 9-month lead times. This is most likely due to a combination of thicker ice initialization in the cold season and an insufficient melting rate in the warm season. When the model is initialized with a more realistic thinner ice in the Arctic using the CryoSat-2 observations in the CS2_IC experiments, a higher forecast skill is achieved in both SIE and SIV at all lead times. Nevertheless, there is still a positive SIV bias in summer in the CS2_IC experiments at 3- to 6-month lead times. More details can be seen in the regional investigation next.

3.1.3 Regions

Analysis of the sea ice prediction skill is performed in regions defined in https://arctic-roos.org in Fig. 9. For the purpose of this study, we refer to the combination of the Barents, Kara, and Greenland Seas as BKG seas. To investigate the season-dependency of the forecast skill seen earlier, we present regional SIE forecasts in Fig. 10 in the control (solid blue) and CS2_IC (dashed red) experiments throughout the 12-month integrations initialized in April 1 of 2013 to 2017, the period when the AMSR2 observations (circle) are available. The control experiment has a reasonable SIE in all 8 regions in summer and fall, but it overpredicts SIE in the BKG Seas, Baffin Bay and East Siberian Sea in winter at lead times longer than 6 months. In the CS2_IC experiment initialized with a more realistic SIV, the SIE prediction is improved in the East Siberian Sea at lead times above 6 months while it remains unchanged in the BKG seas and Baffin Bay.

Regional SIV forecasts from the same experiments in Fig. 10 are shown in Fig. 11, together with the CryoSat-2 observations. The positive SIV bias in the Beaufort, Chukchi, East Siberian and Laptev Seas seen in the control experiment is reduced in the CS2_IC experiments at almost all lead times, indicating that the positive SIV bias in the initialization is mostly responsible for the positive SIV bias in the seasonal forecast in this Arctic region between 120°E and 120°W. Apparently, positive biases in SIE in the BKG Seas and Baffin Bay, all in the vicinity of the Atlantic, come from a different source. It is most likely from the lack of interaction with the Atlantic Ocean, a mechanism which in the current experiments is inadequately simulated by using a simplified mixed layer model mentioned earlier. Without northward oceanic heat transport, the sea ice edge tends to extend too far south in winter.

https://doi.org/10.5194/egusphere-2022-1368
Preprint. Discussion started: 19 December 2022

4 Discussion

In this study, we evaluate sea ice prediction skill at seasonal time scales using the CICE sea ice model in standalone mode, driven by a built-in mixed layer ocean model and atmospheric forcings from the NCEP CFSR reanalysis. The control experiments are initialized with the CFSR reanalysis for both ocean and ice states. Multiple year-long experiments are carried out at monthly interval initialization. The model does a credible job in forecasting SIE in the warm season both in the Arctic and Antarctic at lead times up to 12 months. The biggest bias in the SIE seasonal forecast is in boreal late winter and early spring in the Arctic, and in austral spring in the Antarctic, which limits the seasonal prediction skill of CICE in standalone mode.

We found one of the factors restraining the model forecast skill in the Arctic is the positive SIT bias in the initialization in the control experiments: the initial SIT from CFSR is consistently higher than the CryoSat-2 satellite observations and the excessive ice thickness is often retained for more than one season. We are able to reduce this bias in the CS2_IC experiments by initializing sea ice thickness using the CryoSat-2 satellite observations, while keeping everything else unchanged. Although the CryoSat-2 ice thickness data are only available from October to April in the Arctic, the multi-year experiments initialized with this dataset clearly show the bias reduction in both SIE and SIV at most lead times in almost all seasons.

There are still forecast biases in the CS2_IC experiments. One likely source is in the uncoupled experimental setup, where a simplified column mixed layer model is used, which excludes northward heat transport from both Atlantic and Pacific Oceans. Other possible sources could arise from the prescribed atmospheric forcings, uncertainties in the CryoSat-2 dataset especially over thin ice, or limitations in the CICE model itself. We are unable to identify these in the present setup. This would be a subject of future experiments.

Results presented here are consistent with those in the current NOAA operational seasonal forecast model CFSv2 (Wang et al., 2013), the coupled model in charge of producing the atmospheric reanalysis used to force the CICE experiments here. The RMSE shown in Fig. 2 here is larger than in Wang et al. (2013) for a number of likely reasons: (1) the latter is from a fully coupled model allowing feedback between atmosphere, ocean and sea ice, while this study uses an uncoupled sea ice model with prescribed boundary conditions which may contain errors and are not always 'in tune' with the sea ice model; (2) both the ocean model and the sea ice model are different; (3) the validation period is different. Wang et al. (2013) compared to the 26-year climatology of 1981-2007, while the 2011-2017 period used in this study is characterized by a smaller observed sea ice area than in earlier decades.

This study confirms the importance of the accuracy in ice thickness initialization for seasonal sea ice prediction. It suggests that there exists a potentially important source of additional skill in seasonal forecasting, namely, a more reliable sea ice thickness initialization. Hence, assimilation of sea ice thickness, either from observations or reanalysis, appears to be highly relevant for advancing seasonal prediction skill.

Author contributions. SS and AS designed the study, performed the analyses and wrote the manuscript. SS carried out the numerical experiments and did the first draft of the analyses.

https://doi.org/10.5194/egusphere-2022-1368
Preprint. Discussion started: 19 December 2022

Competing interests. The authors declare that they have no conflicts of interest.

Acknowledgements. This research is funded by the Global Model Test Bed at Developmental Testbed Center under NGGPS. We thank David Bailey for helpful discussions and sharing a script to convert initial conditions to restart conditions for CICE, Xingren Wu for suggesting using a mixed layer ocean instead of SST from CFSv2 and Rainer Bleck for constructive suggestions during the interval review. Discussions with James Rosinski, Ola Persson, Julie Schramm, Janet Intrieri, Chris Fairall, Antonietta Capotondi and Ligia Bernardet are also much appreciated. Benjamin W. Green helped with graphics. The authors would like to express their gratitude to the three anonymous reviewers for their valuable comments, which improved the quality of this manuscript. CFSR data used here are from the Research Data Archive, managed by the Computational and Information Systems Laboratory at the National Center for Atmospheric Research in Boulder, Colorado. The ice concentration data is obtained from the National Snow and Ice Data Center (NSIDC; http://nsidc.org/data/docs/daac/nsidc0051_gsfc_seaice.gd.html).

https://doi.org/10.5194/egusphere-2022-1368
Preprint. Discussion started: 19 December 2022

References

ACIA: Arctic Climate Impact Assessment. ACIA Overview report, Cambridge University Press, Cambridge, U. K., 2005.

Allard, R. A., Farrell, S. L., Hebert, D. A., Johnston, W. F., Li, L., Kurtz, N. T., Phelps, M. W., Posey, P. G., Tilling, R., Ridout, A., and Wallcraft, A. J.: Utilizing CryoSat-2 sea ice thickness to initialize a coupled ice–ocean modeling system, Adv. Space Res., 62, 1265–1280, 2018.

Amante, C. and Eakins, B. W.: ETOPO1 1 Arc-Minute Global Relief Model: Procedures, Data Sources and Analysis, NOAA Technical Memorandum NESDIS NGDC-24, National Geophysical Data Center, NOAA, Available at https://doi.org/10.7289/V5C8276M, 2009.

Blanchard-Wrigglesworth, E., Bitz, C. M., and Holland, M. M.: Influence of initial conditions and climate forcing on predicting Arctic sea ice, Geophysical Research Letters, 38, L18 503, 2011a.

Blanchard-Wrigglesworth, E., Armour, K., Bitz, C. M., and DeWeaver, E.: Persistence and inherent predictability of Arctic sea ice in a GCM ensemble and observations, Journal of Climate, 24, 231–250, 2011b.

Bleck, R. and Sun, S.: Diagnostics of the oceanic thermohaline circulation in a coupled climate model, Global and Planetary Change, 40, 233–248, 2004.

Blockley, E. W. and Peterson, K. A.: Improving Met Office seasonal predictions of Arctic sea ice using assimilation of CryoSat-2 thickness, The Cryosphere, 12, 3419–3438, https://doi.org/10.5194/tc-12-3419-2018, 2018.

Bushuk, M., Msadek, R., Winton, M., Vecchi, G., Yang, X., Rosati, A., and Gudgel, R.: Regional Arctic sea–ice prediction: potential versus operational seasonal forecast skill, Climate Dynamics, 52, 2721–2743, 2019.

Bushuk, M., Winton, M., Bonan, D. B., Blanchard-Wrigglesworth, E., and Delworth, T. L.: A mechanism for the Arctic sea ice spring predictability barrier, Geophysical Research Letters, 47, 1–13, 2020.

Chapman, W. and Walsh, J.: Observed climate change in the Arctic, updated from Chapman and Walsh, 1993, Bulletin of the American Meteorological Society, 74, 33–47, 2003.

Chevallier, M. and Salas-Mélia, D.: The role of sea ice thickness distribution in the Arctic sea ice potential predictability: A diagnostic approach with a coupled GCM, Journal of Climate, 25, 3025–3038, 2012.

Chevallier, M., Smith, G. C., Dupont, F., Lemieux, J.-F., Forget, G., Fujii, Y., Hernandez, F., Msadek, R., Peterson, K. A., Storto, A., Toyoda, T., Valdivieso, M., Vernieres, G., Zuo, H., Balmaseda, M., Chang, Y.-S., Ferry, N., Garric, G., Haines, K., Keeley, S., Kovach, R. M., Kuragano, T., Masina, S., Tang, Y., Tsujino, H., and Wang, X.: Intercomparison of the Arctic sea ice cover in global ocean–sea ice reanalyses from the ORA-IP project, Journal of Climate, 49, 1107–1136, https://doi.org/10.1007/s00382-016-2985-y, 2017.

Collow, T. W., Wang, W. Q., Kumar, A., and Zhang, J. L.: Improving Arctic Sea Ice Prediction Using PIOMAS Initial Sea Ice Thickness in a Coupled Ocean-Atmosphere Model, Monthly Weather Review, 143(11), 4618–4630, 2015.

Day, J. J., Hawkins, E., and Tietsche, S.: Will Arctic sea ice thickness initialization improve seasonal forecast skill?, Geophysical Research Letters, 41, 7566–7575, 2014a.

Day, J. J., Tietsche, S., and Hawkins, E.: Pan-Arctic and regional sea ice predictability: Initialization month dependence, Journal of Climate, 27, 4371–4390, 2014b.

Dethloff, K., Rinke, A., Benkel, A., Køltzow, M., Sokolova, E., Saha, S. K., Handorf, D., Dorn, W., Rockel, B., von Storch, H., Haugen, J. E., Røed, L. P., Roeckner, E., Christensen, J. H., and Stendel, M.: A dynamical link between the Arctic and the global climate system, Geophysical Research Letters, 33, L03 703, 2006.

https://doi.org/10.5194/egusphere-2022-1368
Preprint. Discussion started: 19 December 2022

Dirkson, A., Merryfield, W. J., and Monahan, A.: Impacts of Sea Ice Thickness Initialization on Seasonal Arctic Sea Ice Predictions, Journal of Climate, 30, 1001–1017, https://doi.org/doi.org/10.1175/JCLI-D-16-0437.1, 2017.

Grosfeld, K., Treffeisen, R., Asseng, J., Bartsch, A., Bräuer, B., Fritzsch, B., Gerdes, R., Hendricks, S., Hiller, W., Heygster, G., Krumpen, T., Lemke, P., Melsheimer, C., Nicolaus, M., Ricker, R., and Weigelt, M.: Online sea-ice knowledge and data platform <www.meereisportal.de>, Polarforschung, 85, 143–155, 2016.

Grumbine, R.: Long Range Sea Ice Drift Model Verification, MMAB Tech Note, 315, 22 pp, 2003.

Guemas, V., Blanchard-Wrigglesworth, E., Chevallier, M., Day, J. J., Déqué, M., Doblas-Reyes, F. J., Fučkar, N. S., Germe, A., Hawkins, E., Keeley, S., Koenigk, T., y Mélia, D. S., and Tietschee, S.: A review on Arctic sea-ice predictability and prediction on seasonal to decadal time-scales, Q. J. R. Meteorol. Soc., 142, 546–561, https://doi.org/10.1002/qj.2401, 2016.

Hebert, D. A., Allard, R. A., Metzger, E. J., Posey, P. G., Preller, R. H., Wallcraft, A. J., Phelps, M. W., and Smedstad, O. M.: Short-term sea ice forecasting: an assessment of ice concentration and ice drift forecasts using the u.s. navy's arctic cap nowcast/forecast system, J. Geophys. Res. Oceans, 120, 1–19, 2015.

Holland, M. M. and Bitz, C. M.: Polar amplification of climate change in coupled models, Climate Dynamics, 21, 221–232, 2003.

Holland, M. M., Bailey, D. A., and Vavrus, S.: Inherent sea ice predictability in the rapidly changing arctic environment of the community climate system model, version 3, Climate Dynamics, 36, 1239–1253, 2011.

Hunke, E., Allard, R., Blain, P., et al.: Should Sea-Ice Modeling Tools Designed for Climate Research Be Used for Short-Term Forecasting?, Curr Clim Change Rep, 6, 121–136, 2020.

Hunke, E. C., Lipscomb, W. H., Turner, A. K., Jeffery, N., and Elliott, S.: CICE: the Los Alamos sea ice model documentation and software user's manual version 5.1, 2015.

Intrieri, J. M., Solomon, A., Cox, C., Persson, O., de Boer, G., Hughes, M., and Capotondi, A.: Sub-seasonal forecasting of the coupled Arctic system: Evaluation of the NOAA Experimental Coupled Arctic Forecast System (CAFS), manuscript to be submitted, 2022.

IPCC: Climate Change 2014: Synthesis Report, Contribution of Working Groups I, II and III to the Fifth Assessment Report of the Intergovernmental Panel on Climate Change [Core Writing Team, R.K. Pachauri and L.A. Meyer (eds.)]. IPCC, Geneva, Switzerland, 2014.

IPCC: Summary for Policymakers. In: Climate Change 2021: The Physical Science Basis, Contribution of Working Group I to the Sixth Assessment Report of the Intergovernmental Panel on Climate Change [Masson-Delmotte, V., P. Zhai, A. Pirani, S. L. Connors, C. Péan, S. Berger, N. Caud, Y. Chen, L. Goldfarb, M. I. Gomis, M. Huang, K. Leitzell, E. Lonnoy, J.B.R. Matthews, T. K. Maycock, T. Waterfield, O. Yelekçi, R. Yu and B. Zhou (eds.)]. Cambridge University Press. In Press, 2021.

Jaiser, R., Dethloff, K., Handorf, D., Rinke, A., and Cohen, J.: Impact of sea ice cover changes on the Northern Hemisphere atmospheric winter circulation, Tellus A: Dynamic Meteorology and Oceanography, 64, 11 595, 2012.

Krinner, G., Rinke, A., Dethloff, K., and Gorodetskaya, I.: Impact of prescribed Arctic sea ice thickness in simulations of the present and future climate, Climate Dynamics, 35, 619–633, 2010.

Laxon, S. W., Giles, K. A., Ridout, A. L., Wingham, D. J., Willatt, R., Cullen, R., Kwok, R., Schweiger, A., Zhang, J., Haas, C., Hendricks, S., Krishfield, R., Kurtz, N., Farrell, S., and Davidson, M.: CryoSat-2 estimates of Arctic sea ice thickness and volume, Geophys. Res. Lett., 40, 732–737, 2013.

Li, X., Gerber, D. M. H. E. P., and Yoo, C.: Impacts of the north and tropical Atlantic Ocean on the Antarctic Peninsula and sea ice, Nature, 505, 538–542, 2014.

Liu, J., Song, M., Horton, R. M., and Hu, Y.: Revisiting the potential of melt pond fraction as a predictor for the seasonal Arctic sea ice extent minimum, Environ. Res. Lett., 10, 054 017, 2015.

https://doi.org/10.5194/egusphere-2022-1368
Preprint. Discussion started: 19 December 2022

Meier, W. N., Stroeve, J., Barrett, A., and Fetterer, F.: A simple approach to providing a more consistent arctic sea ice extent time series from the 1950s to present, Cryosphere, 6, 1359–1368, 2012.

Randall, D., Curry, J., Battisti, D., Flato, G., Grumbine, R., Hakkinen, S., Martinson, D., Preller, R., Walsh, J., , and Weatherly, J.: Status of and Outlook for Large-Scale Modeling of Atmosphere–Ice–Ocean Interactions in the Arctic, Bulletin of the American Meteorological Society, 79, 197–220, 1998.

Ricker, R., Hendricks, S., Helm, V., Skourup, H., and Davidson, M.: Sensitivity of CryoSat-2 Arctic sea-ice freeboard and thickness on radar-waveform interpretation, The Cryosphere, 8, 1607–1622, 2014.

Ricker, R., Hendricks, S., Kaleschke, L., Tian-Kunze, X., King, J., and Haas, C.: A weekly Arctic sea-ice thickness data record from merged CryoSat-2 and SMOS satellite data, The Cryosphere, 11, 1607–1623, 2017.

Roberts, A., Craig, A., Maslowski, W., Osinski, R., Duvivier, A., Hughes, M., Nijssen, B., Cassano, J., and Brunke, M.: Simulating transient ice-ocean Ekman transport in the Regional Arctic System Model and Community Earth System Model. 211-228. doi:10.3189/2015AoG69A760, Annals of Glaciology, 56, 211–228, 2015.

Saha, S., Moorthi, S., Pan, H.-L., Wu, X., Wang, J., Nadiga, S., Tripp, P., Kistler, R., Woollen, J., Behringer, D., Liu, H., Stokes, D., Grumbine, R., Gayno, G., Wang, J., Hou, Y.-T., ya Chuang, H., Juang, H.-M. H., Sela, J., Iredell, M., Treadon, R., Kleist, D., Delst, P. V., Keyser, D., Derber, J., Ek, M., Meng, J., Wei, H., Yang, R., Lord, S., van den Dool, H., Kumar, A., Wang, W., Long, C., Chelliah, M., Xue, Y., Huang, B., Schemm, J.-K., Ebisuzaki, W., Lin, R., Xie, P., Chen, M., Zhou, S., Higgins, W., Zou, C.-Z., Liu, Q., Chen, Y., Han, Y., Cucurull, L., Reynolds, R. W., Rutledge, G., and Goldberg, M.: NCEP Climate Forecast System Reanalysis, Bulletin of the American Meteorological Society, 91, 1015–1058, 2010.

Schröder, D., Feltham, D. L., Tsamados, M., Ridout, A., and Tilling, R.: New insight from CryoSat-2 sea ice thickness for sea ice modelling, The Cryosphere, 13, 125–139, 2019.

Schweiger, A., Lindsay, R., Zhang, J., Steele, M., and Stern, H.: Uncertainty in modeled arctic sea ice volume, J. Geophys. Res., 116, C00D06, 2011.

Spreen, G., Kaleschke, L., and Heygster, G.: Sea ice remote sensing using AMSR-E 89 1448 GHz channels, J. Geophys. Res., 113, C02S03, 2008.

Wang, W., Chen, M., and Kumar, A.: Seasonal prediction of Arctic sea ice extent from a coupled dynamical forecast system, Monthly Weather Review, 141, 1375–1394, 2013.

https://doi.org/10.5194/egusphere-2022-1368
Preprint. Discussion started: 19 December 2022

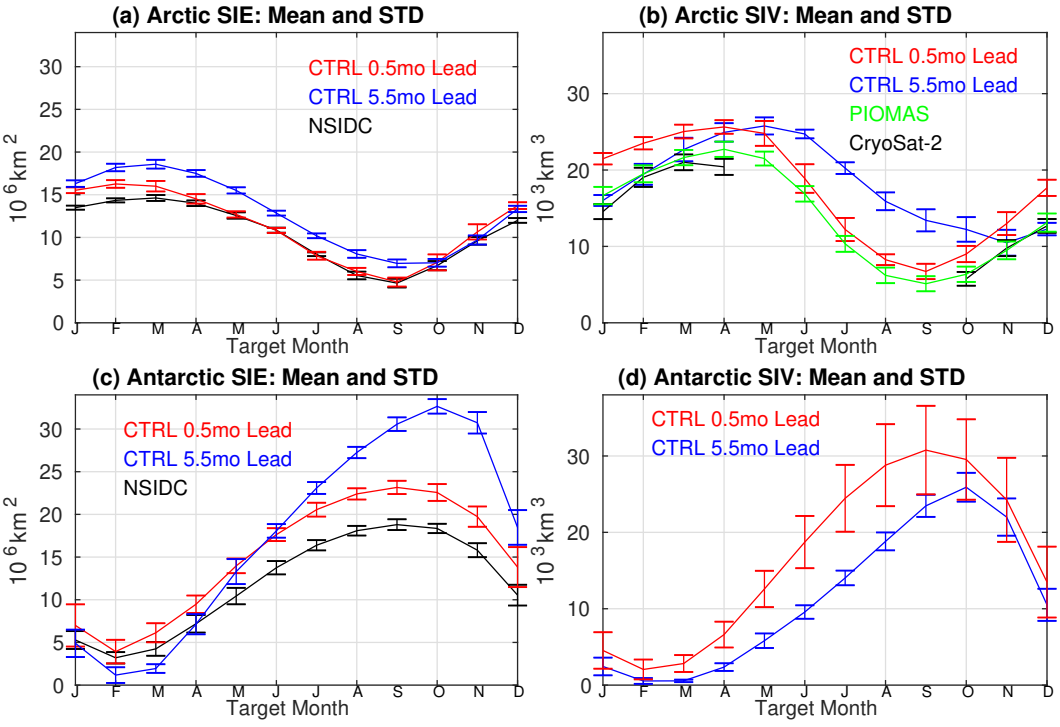

Figure 1. Upper: the mean and standard deviation of sea ice extent (SIE) at each target month from forecasts at 0.5-month and 5.5-month lead times in the control experiments and NSIDC observations. Averaged over 2011-2017. Lower: same as upper, except for sea ice volume (SIV) with CryoSat-2 observations and PIOMAS reanalysis. Left: Arctic; Right: Antarctic.

https://doi.org/10.5194/egusphere-2022-1368
Preprint. Discussion started: 19 December 2022

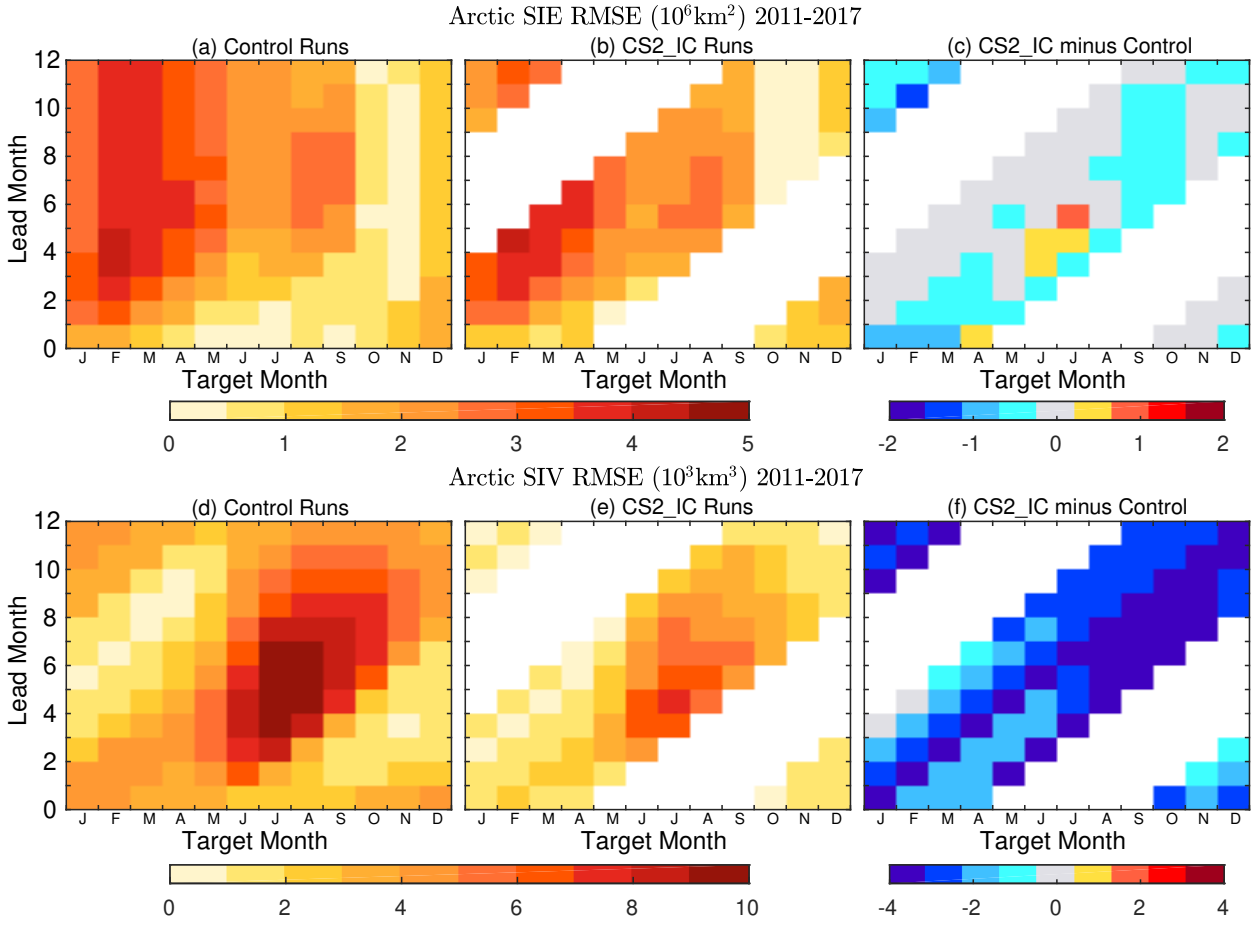

Figure 2. Upper: root mean square error (RMSE) in the Arctic sea ice extent (10^6 km^2) with respect to NSIDC at lead times up to 12 months against target month in the control [left, (a)] and in the CS2_IC experiments [middle, (b)] and the difference of (b) and (a) (right). Averaged over 2011-2017. Lower: same as upper, except for sea ice volume (10^3 km^3) w.r.t. PIOMAS. White spaces indicate no model data due to lack of CryoSat-2 data for model initialization from May to September.

https://doi.org/10.5194/egusphere-2022-1368
Preprint. Discussion started: 19 December 2022

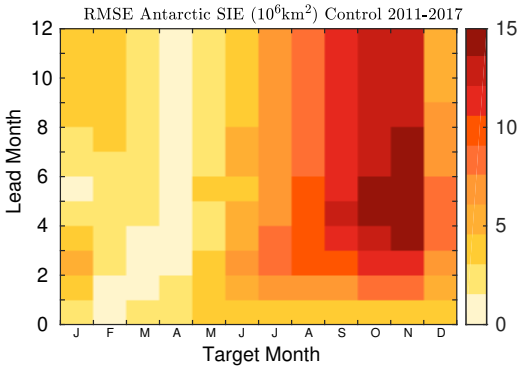

Figure 3. RMSE in the Antarctic sea ice extent w.r.t. NSIDC in the control experiments at lead times up to 12 months against target month. Averaged over 2011-2017.

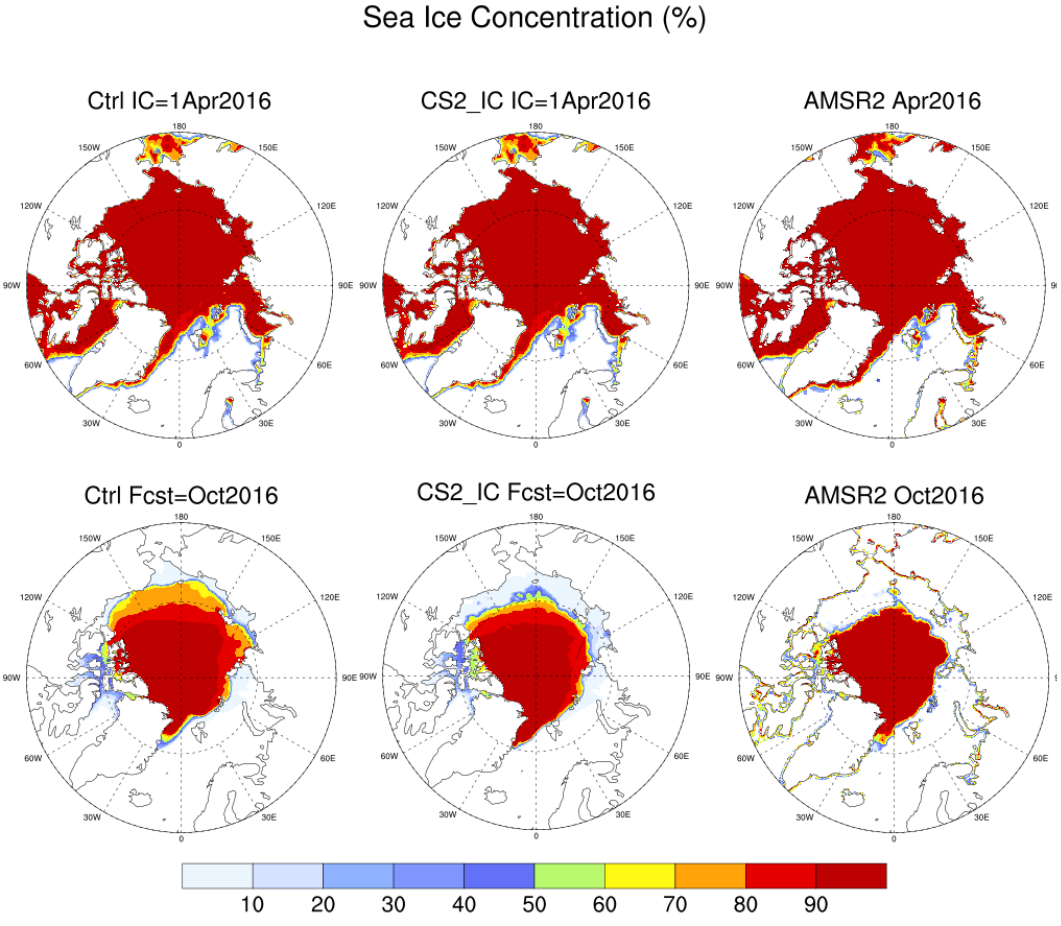

Figure 4. Arctic sea ice concentration (%). Left: initial condition on April 1, 2016 and forecast for October 2016 in the control experiment; Middle: same as left, except in the CS2_IC experiments; Right: corresponding AMSR2 observations.

https://doi.org/10.5194/egusphere-2022-1368
Preprint. Discussion started: 19 December 2022

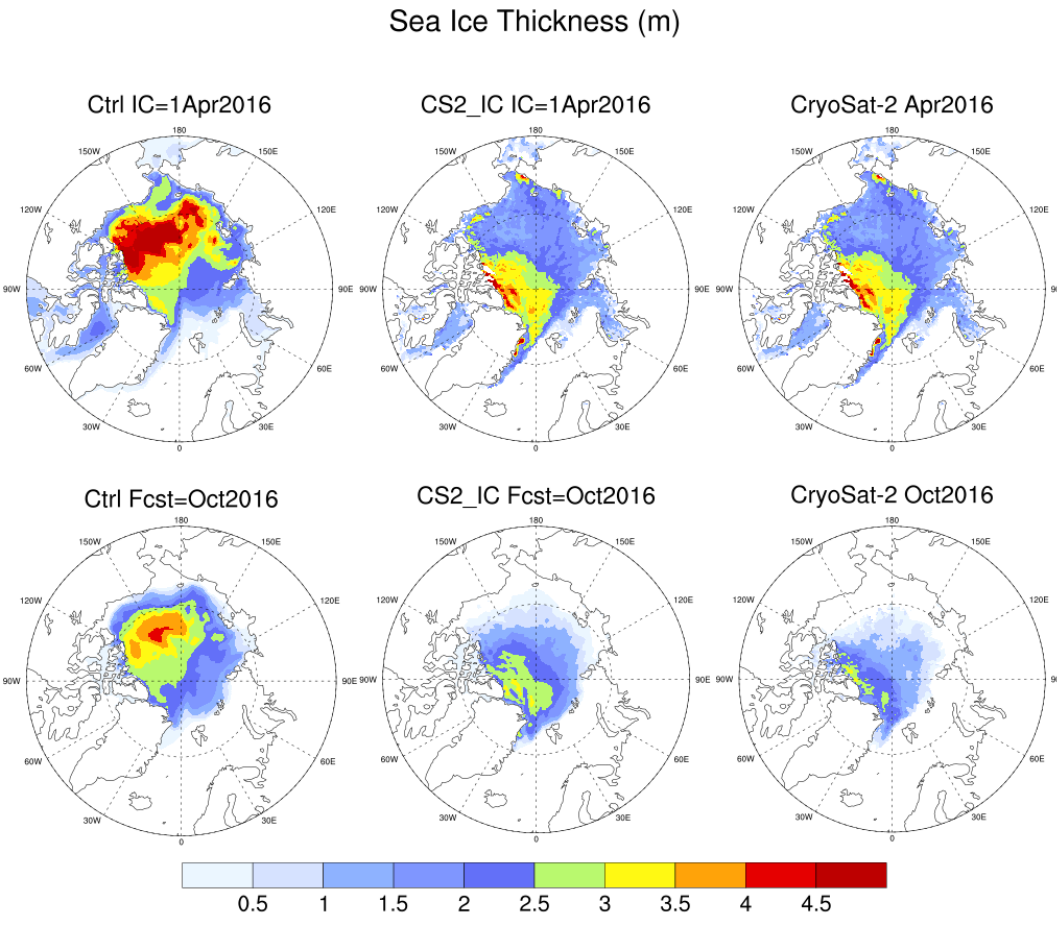

Figure 5. Same as Fig. 4, except for sea ice thickness (m) with CryoSat-2 observations.

https://doi.org/10.5194/egusphere-2022-1368
Preprint. Discussion started: 19 December 2022

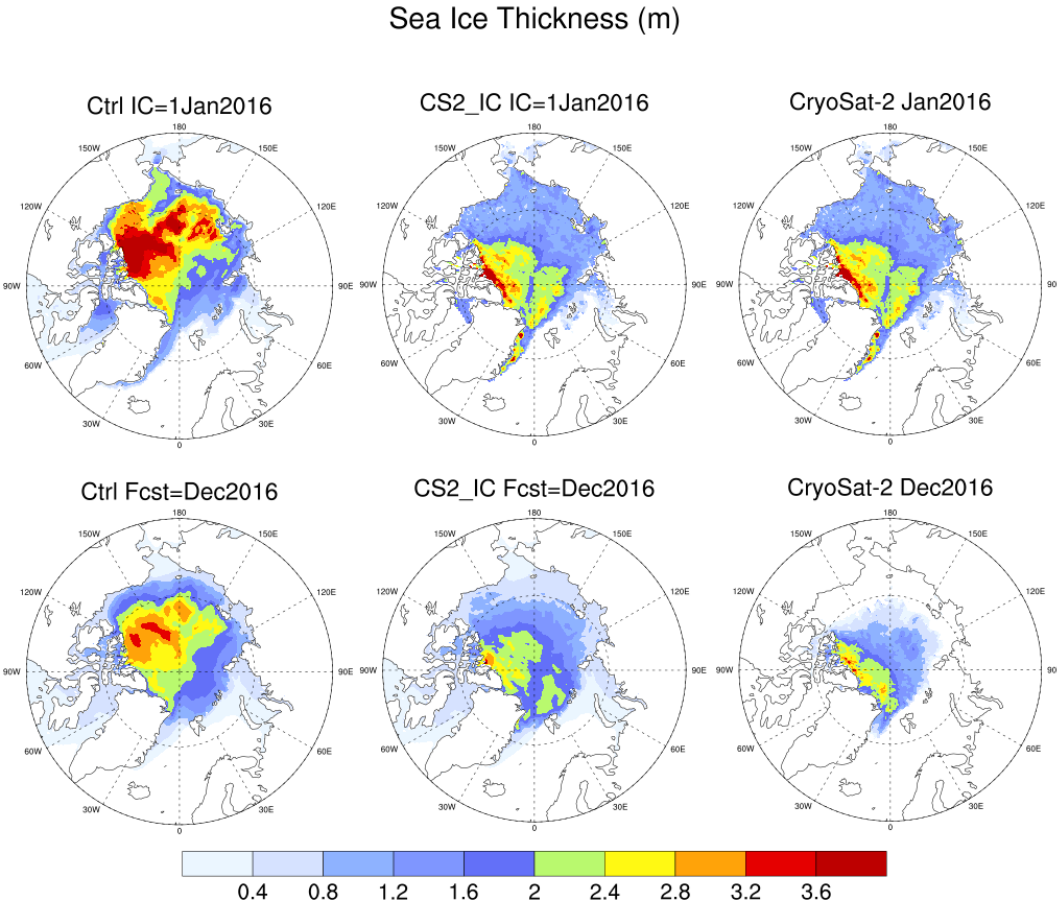

Figure 6. Arctic sea ice thickness (m). Left: initial condition on January 1, 2016 and forecast for December 2016 in the control experiment; Middle: same as left, except in the CS2_IC experiments; Right: corresponding CryoSat-2 observations.

https://doi.org/10.5194/egusphere-2022-1368
Preprint. Discussion started: 19 December 2022

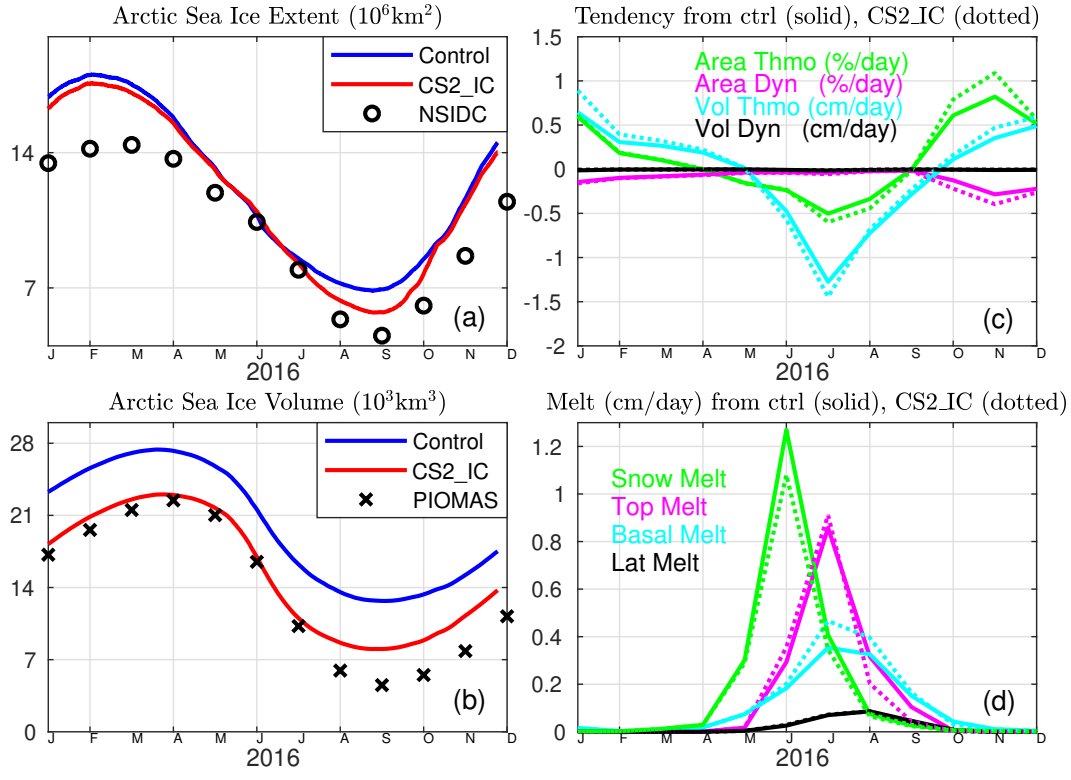

Figure 7. Forecasts of Arctic sea ice extent and sea ice volume up to 12 months initialized on January 1, 2016 in the control and CS2_IC experiments are in (a) and (b) in comparison with NSIDC observations and PIOMAS reanalysis. The corresponding tendency of SIE (%/day) and SIV (cm/day) attributed to ice thermodynamics and dynamics are in (c), and melting rates (cm/day) from snow, top, basal and lateral are in (d) in the control (solid) and CS2_IC (dotted) experiments. Averages north of 67.5°N are shown in (c) and (d).

https://doi.org/10.5194/egusphere-2022-1368
Preprint. Discussion started: 19 December 2022

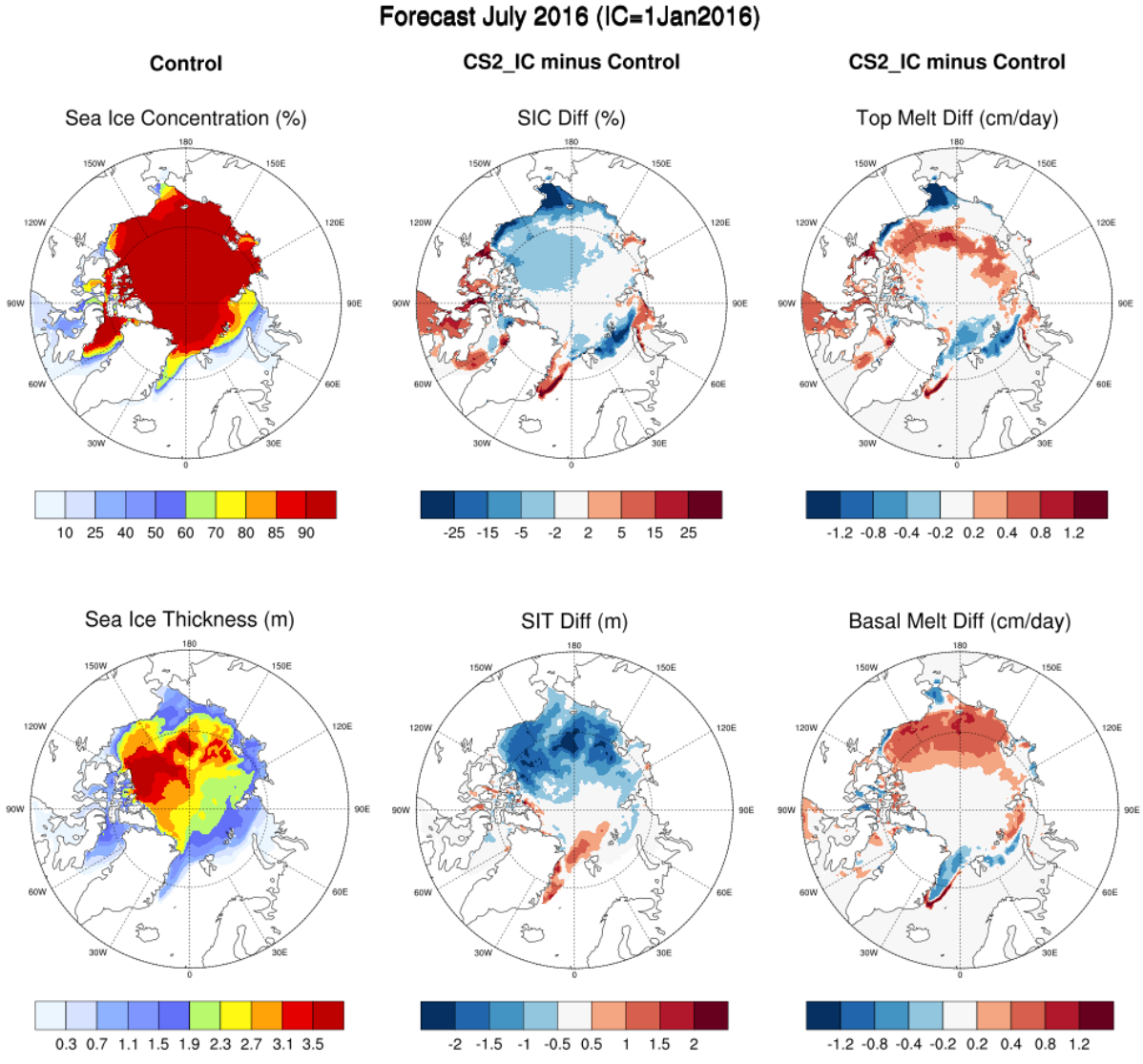

Figure 8. Arctic sea ice concentration (%) and sea ice thickness (m) in the control experiment are shown in the left column. The difference between CS2_IC and control experiments in the sea ice concentration (%), sea ice thickness (m), the top and basal melting rates (cm/day) are in the middle and right columns. All are forecast for July 2016 initialized on January 1, 2016.

https://doi.org/10.5194/egusphere-2022-1368
Preprint. Discussion started: 19 December 2022

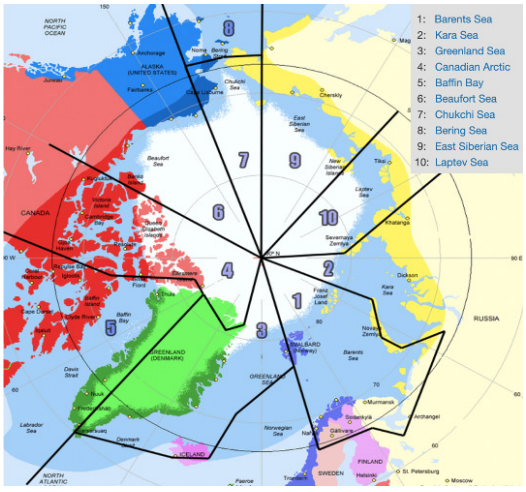

Figure 9. Different regions in the Arctic Ocean. Reproduced from https://arctic-roos.org.

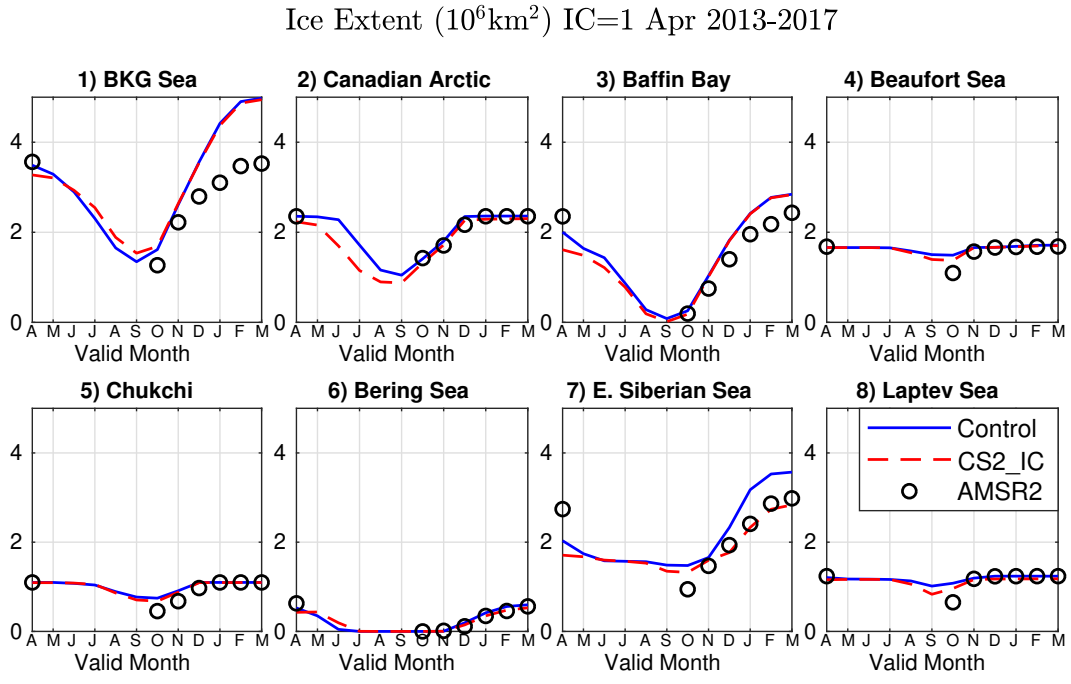

Figure 10. Sea ice extent during 12-month integration in the control (solid blue) and CS2_IC (dashed red) experiments, initialized in April 2013 to 2017, and AMSR2 observations (circles) in each region where (1) represents Barents, Kara and Greenland Seas (BKG) combined.

https://doi.org/10.5194/egusphere-2022-1368
Preprint. Discussion started: 19 December 2022

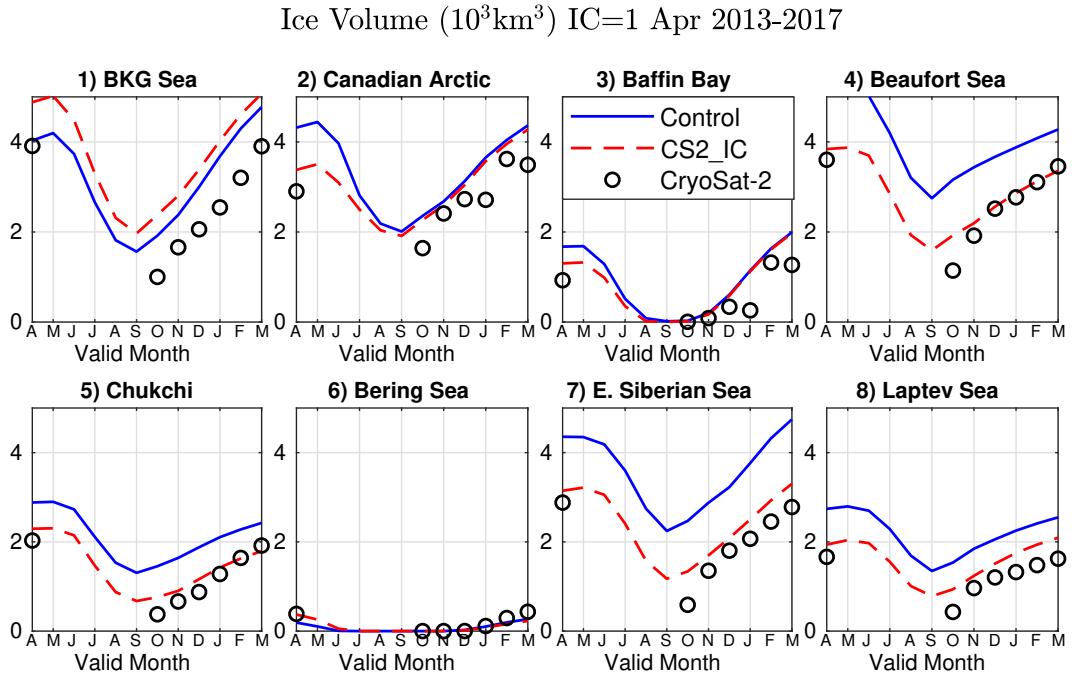

Figure 11. Same as Fig. 10, except for SIV where circles mark CryoSat-2 observations.